A SINGLE-PHASE GRID-CONNECTED PV SYSTEM WITH ACTIVE POWER FILTER

Kleber C. A. de Souza, Roberto F. Coelho, Felipe Valore, Denizar C. Martins
Federal University of Santa Catarina, Department of Electric Engineering, Power Electronic Institute
P.O. Box: 5119, Zip Code: 88040-970, Florianópolis, SC – Brazil
ksouza@inep.ufsc.br, roberto@inep.ufsc.br, valore@inep.ufsc.br, denizar@inep.ufsc.br

***Abstract* – A single-phase grid-connected photovoltaic system with active power filter is presented. Depending on the solar radiation, the system can work as generator or as an active power line conditioning. Besides, just using a sensor one, the control strategy is simpler and of easy practical implementation. Even with the connection of a load between the grid and the system, the output current will be in phase with the utility and a unity power factor is obtained.**

***Keywords* – Single-phase, PV systems and active power filter.**

I. INTRODUCTION

Inverters for photovoltaic (PV) applications have to contain some basic functionalities. The conversion of the low voltage generated at the MPP (typically around 17 V for a 36 cells module and 34 V for a 72 cells module) to a corresponding AC current injected into the grid, must be done with the highest possible efficiency over a wide range of PV-power. This requirement is given due to the irradiation distribution of the sun.

In almost all works published in the area, the stage connected to the network is made up of a full bridge inverter towards the grid, either grid-commutated at twice the grid-frequency (120Hz) [1-2] (Fig. 1) or self-commutated with a high switching frequency [3-4] (Fig. 2).

Benefits for the grid-commutated solution are that the switching losses from the stage are completely removed and only the conduction losses remain. This means that the grid current must be sine-modulated in another sense, e.g. by the DC-DC converter. On the other hand, if a DC-DC converter is used in a self-commutated inverter it has a function of just amplifying the array voltage and to follow the maximum power condition of the panel. If the self-commutated system uses only a DC-AC converter [5], it is connected directly to the photovoltaic array which is configured in such a way to attend voltage and current specification.

Thus, this paper presents a study of a PV energy conversion system controlled so as to supply power to the load and supply surplus power with a unity power factor to the utility line. Simultaneously, the system must be operated so as to track the maximum power point of the PV array. The structure is a two stages system, but can be adapted to work connected directly to the photovoltaic array.

II. SYSTEM CONFIGURATION AND CONTROL

Fig. 3 presents the full bridge topology with the inductor L connected between the grid ($V_o(t)$) and the inverter, the capacitor C_i in the structure input representing the DC voltage source and a current source ($I_i(t)$), that can be either the output of the DC-DC converter or an array of photovoltaic panels.

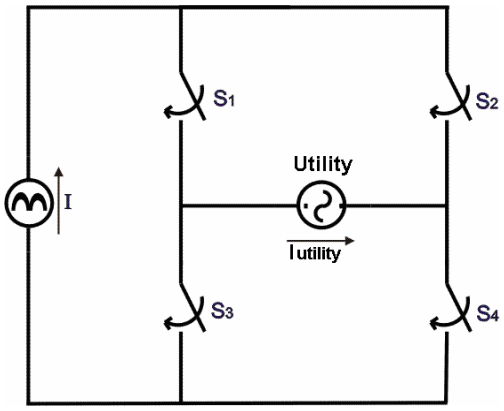

Fig. 1 Current feed, grid-commutated inverter switching at twice the grid frequency.

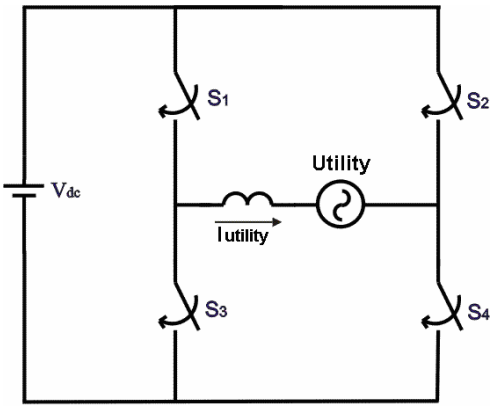

Fig. 2. Voltage feed, self-commutated inverter switching at high frequency.

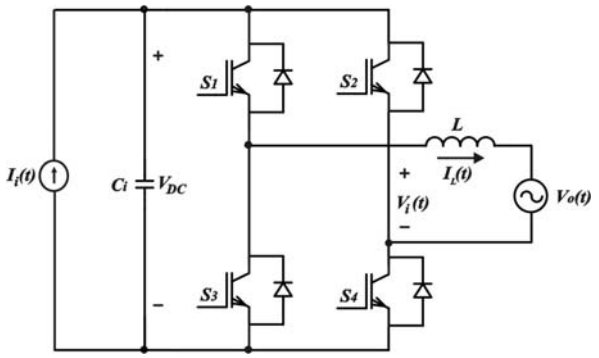

Fig. 3. Full bridge inverter.

Considering the self-commutated inverter switching at high frequency and using three level PWM technique, it is possible to represent the four equivalent circuits of the switching modes (Fig. 4), defined by the combination of the switches possible states with the two possible direction of the output current.

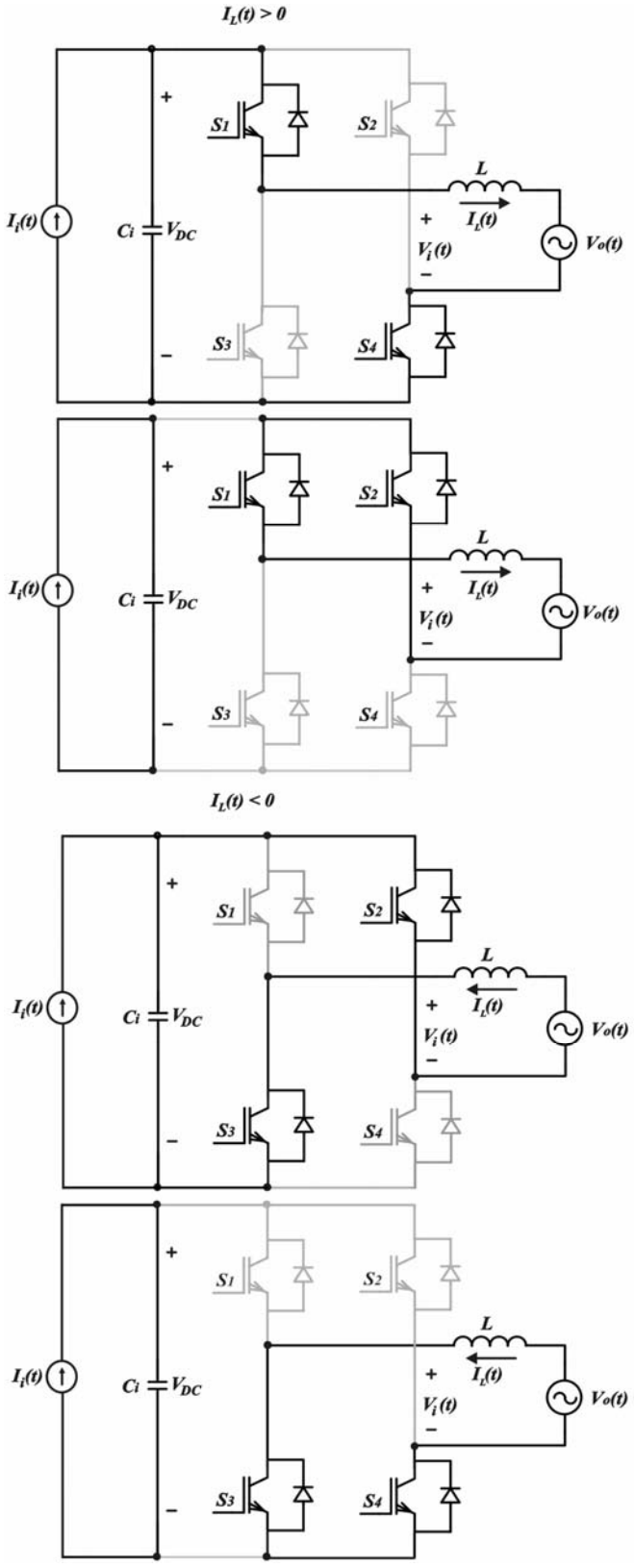

Fig. 4. Simplified four equivalent circuits of the switching modes.

From the operational stages, it can be observed that when $I_L(t)>0$ and the switches S_1 e S_4 are on, voltage $V_i(t)$ has its polarity defined by the direction of the output current, with its absolute value equal to input voltage V_{DC}, whose amplitude should be larger than the peak value of the output voltage, $V_o(t)$. In this manner, the voltage polarity across the inductor causes its current's absolute value to increase. During this stage, energy from the input source, V_{DC}, along with part of the energy stored in the inductor, is transferred to the grid. When $I_L(t)>0$ and the switches S_1 e S_3 are on, voltage $V_i(t)$ is zero. In this manner, the voltage polarity across the inductor is inverted, causing its current's absolute value to decrease. Indeed, the output current is controlled by imposing the derivative of the current through the inductor, or, put differently, by imposing the voltage across the inductor L. In this manner, the structure of the converter shown in Fig. 3 can be represented, without loss of generality, as the controlled voltage source $V_i(t)$, presented in Fig. 5.

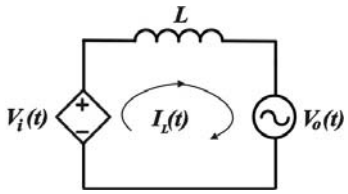

Fig. 5. Simplified equivalent circuit.

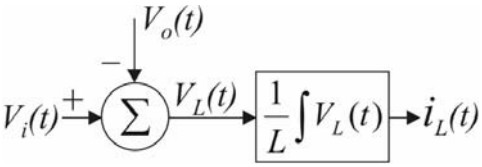

Fig. 6. Block diagram of the simplified equivalent circuit.

In Fig. 5 the energy flow is controlled by the current $I_L(t)$. However, this current is defined by the difference of voltage between the sources $V_i(t)$ and $V_o(t)$, applied across the impedance. In this case, as the impedance is a pure inductance, the current will be equal the integral of the voltage across it. As $V_o(t)$ is known, once it is the utility voltage itself, $V_i(t)$ is imposed and therefore $V_L(t)$, in a convenient form, in a way to obtain the output current desired across the inductor. Thus,

$$V_L(t) = L \cdot \frac{dI_L(t)}{dt} \text{ or } I_L(t) = \frac{1}{L} \cdot \int V_L(t) \cdot dt \quad (1)$$

$$V_L(t) = V_i(t) - V_o(t) \quad (2)$$

PWM defines a modulated signal composed of the reproduction of the modulating signal's spectrum, whose amplitude is defined by the modulation, added to harmonic components of frequencies that are multiples of the switching frequency. Ignoring the effect of the harmonic components of the switching frequency on voltage $V_i(t)$, once the inductor works as a low pass filter for the current, the voltage imposed across the inductor is represented simply by (2). Fig. 6 shows the manner in which the converter allows the voltage to be imposed across the inductor, as shown in the equivalent circuit of Fig. 5.

In the classic control strategy, an internal current loop and an external loop to control the input voltage are implemented. The voltage loop defines the amplitude of the reference current by multiplying its control signal by a "waveform", which can be a sample of the output voltage or a digitally generated sinusoid, generating the output current reference. Fig. 7 demonstrates how the classic control strategy is implemented, in which $V_i(t)$ is determined by the current error signal passing through the compensator and the error signal is the difference between a sample of the current and its reference. Fig. 8 shows the same block diagram simplified.

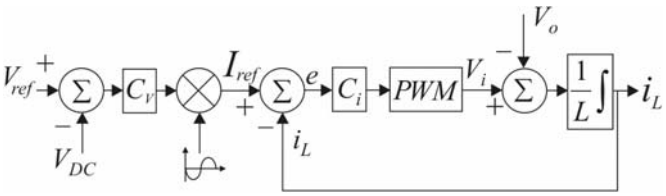

Fig. 7. Block diagram of classical control strategy current loop.

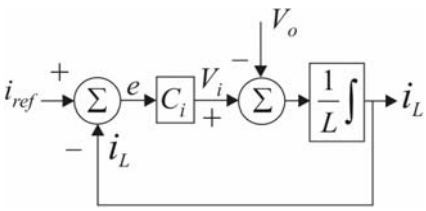

Fig. 8. Simplified block diagram of classical control strategy current loop.

It is observed, however, that the output voltage $V_o(t)$ appears as a disturbance in the simplified traditional model. Therefore, voltage $V_i(t)$, which, in effect, is defined by the control loop should present a sine, in order to annul the effect of $V_o(t)$, and a cosine, which, by composition, will be the resulting voltage imposed across the inductor, therefore, guaranteeing a sinusoidal current. In practice, at the frequency of the mains, the inductor is a very small reactance, causing the voltage drop across the inductor to be much smaller than the voltage of the mains. In other words, the sine of $V_i(t)$ dominates the cosine, demonstrating that the demand on the current loop is much more in favor of annulling the "disturbance" of the output voltage rather than to effectively control the output current.

Rewriting equation (2) as in (3) [6]:

$$L \cdot \frac{di_L(t)}{dt} = k \cdot v_{control}(t) - V_o(t) \quad (3)$$

$$k = \frac{V_{DC}}{V_{tri}} \quad (4)$$

Where V_{tri} is the peak of the triangular carrier signal and $v_{control}$ is the control signal witch shapes the sinusoidal current to the utility line. From the block diagram, the current signal error is equal the equation (5).

$$e(t) = i_{Lref}(t) - i_L(t) \quad (5)$$

Because a perfect sinusoidal current to the utility line is a designed goal, e must naturally approach zero. Thus, deriving (5) and substituting (3) into (6),

$$\frac{de(t)}{dt} = 0 = \frac{di_{Lref}(t)}{dt} - \frac{di_L(t)}{dt} \quad (6)$$

$$v_{control}(t) = \frac{L}{k} \cdot \frac{di_{Lref}(t)}{dt} + \frac{1}{k} \cdot V_o(t) \quad (7)$$

As the disturbance is measurable, the utility voltage disturbance controller G_{cd} is used to reduce de disturbed voltage component. The new block diagram that contains this feed-forward controller is presented in Fig. 9. From Fig. 9, it can be seen that,

$$i_L = \frac{k \cdot C_I}{sL + k \cdot C_I} \cdot I_{Lref} + \frac{k \cdot \left(G_{cd} - 1/k\right)}{sL + k \cdot C_I} \cdot V_o \quad (8)$$

From (8), when $G_{cd} = 1/k$, the disturbance from V_o can be eliminated, and if $kC_i >> |sL|$, than $I_L = I_{ref}$, identifying accurate current control effect for I_{ref}.

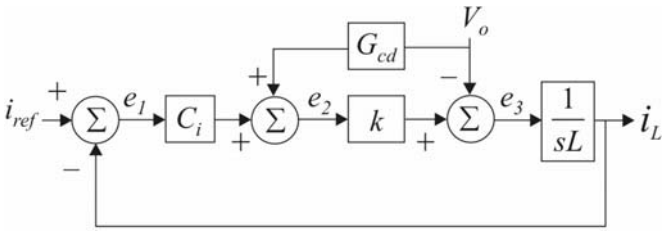

Fig. 9. Block diagram containing the feed-forward controller.

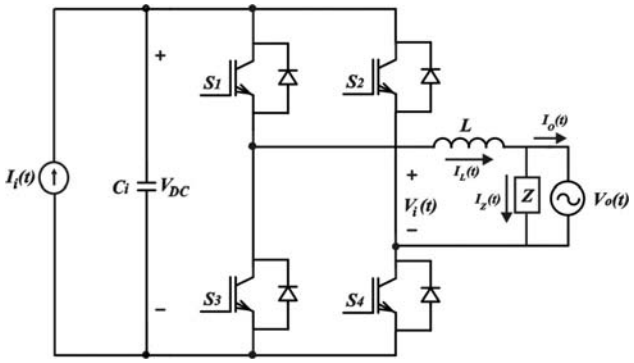

Fig. 10. PV system with any load connected.

Repeating the same analysis, but now considering the connection of any load between the system and the commercial electric grid, a new configuration, presented in Fig. 10, is obtained. It can be observed that now the inductor current is the load current plus the utility current. Again, as sinusoidal current to the utility line is a designed goal, adding a sample of the load current to the inductor current reference it is possible to control the inductor current and still guarantee a sinusoidal utility current. A new block diagram representing the system is shown in Fig. 11.

However, in this case, besides the current sensor used to sample the current in L, it is the necessary another sensor to sample the current in the load. Another disadvantage in this configuration is that as the control is done monitoring the load current (I_Z), when the system is operating Active Power Line Conditioner Mode (low insolation), is necessary before to extract the fundamental component of the load current for

later to find the reference current. So, it is necessary to observe a period of the grid at least.

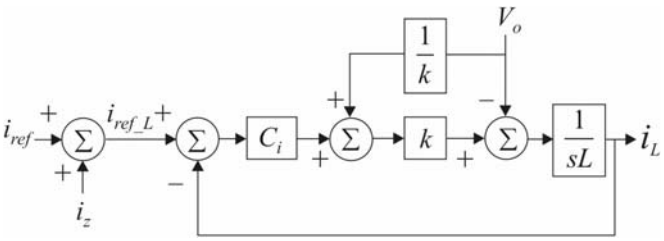

Fig. 11. New block diagram of the inductor current loop.

However, sensing the AC mains current instead of the inductor current, and considering that the difference between the inductor current and the load current is the utility current, the last block diagram can be modified to represent now the utility current loop (Fig. 12). Nevertheless, according to Fig. 7, $i_{o\_ref}(t)$, or, the difference between the reference inductor current (i_{L_ref}) and the load current (I_z), is exactly the own i_{ref} defined by the voltage control signal multiplied by a sinusoid in phase with the utility frequency (Fig. 13). Thus, the same system can be controlled observing only the utility current directly (I_o), improving the dynamics of the same, once it will be not necessary any previous calculation.

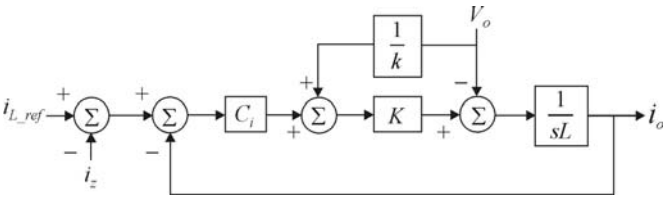

Fig. 12. Block diagram of the utility current loop.

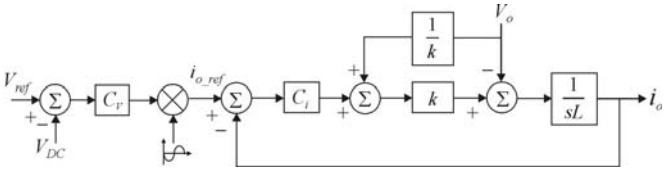

Fig. 13. Utility current control diagram.

Thus, to control the output current in phase with the voltage utility and, to obtain a unity power factor, even with the connection of a load between the grid and the system, it is enough to observe only the AC mains current. In this case, besides doing use of just a sensor one, the control strategy is simpler and of easy practical implementation.

III. SIMULATION RESULTS

To verify the performance of the proposed PV energy conversion system, the following parameters are selected for simulation implementation.

- Input voltage: 400V (DC);
- Output voltage: 220V (AC);
- Input power: 1kW;
- Inverter switching frequency: 20kHz;

The grid-connected system (Fig. 14) was simulated with nonlinear capacitive and nonlinear inductive loads connected between the grind and the system. In Fig. 15 the results illustrate first the currents in the output inductor and in the nonlinear capacitive load following by the utility current with the voltage of the electric system. The utility voltage was divided by thirty to facilitate the visualization. Fig. 16 shows first output inductor current and the nonlinear inductive load current following by the utility current with the voltage of the electric system.

Fig. 17 shows the proposed conversion system switching between solar generator mode and active power mode.

IV. CONCLUSION

The present work presents a study for a design of an inverter, switching in high frequency, to be used in grid-connected photovoltaic systems. The proposed PV system has the advantage of operates in two modes, providing solar generation when insolation is adequate and active power line conditioning when insolation is inadequate. Switching between the two modes is smooth and stable.

The simplicity in the strategy of the output current control, in other words, current injected in the electric system, is another advantage of the study, because besides doing use of just a sensor one, it is of easy practical implementation.

ACKNOWLEDGEMENT

The authors would like to thank the Brazilian agency CNPq for financial support.

REFERENCES

[1] H. Watanabe, T. Shimizu, G. Kimura, “A novel utility interactive photovoltaic inverter with generation control circuit”, *IEEE proc. of 24th IECON*, vol. 02, pp. 721-725, August/September 1998, Germany.

[2] M. Meinhardt, T. O’donnell, H. Schneider, J. Flannery, C. O. Mathuna, P. Zacharias, T. Krieger, “Miniaturised low profile module integrated converter for photovoltaic applications with integrated magnetic components”, IEEE proc. of APEC’99, vol. 01, pp. 305-311, March 1999, EUA.

[3] N. Mohan, T. M. Undeland, W. P. Robbins, Power Electronics: converters, applications, and design, John Wiley & Sons, 2nd Edition, New York, USA, 1995.

[4] S. Saha, V. P. Sundarsingh, “Novel grid-connected photovoltaic inverter”, *IEEE proc. of Generation, Transmission and Distribution*, vol. 143, issue. 2, pp. 219-224, March 1996.

[5] S. W. H. de Haan, H. Oldenkamp, E. J. Wildenbeest, “Test results of a 130 W AC module; a modular solar ac power station”, *IEEE proc. of 1st WCPEC*, pp. 925-928, December 1994, EUA.

[6] Yeong-Chau Kuo, Tsorng-Juu Liang, Jiann-Fuh Chen, “Novel maximum-power-point-tracking controller for photovoltaic energy conversion system”, IEEE Transactions on Industrial Electronics; vol. 48, issue 3, pp. 594-601, June 2001.

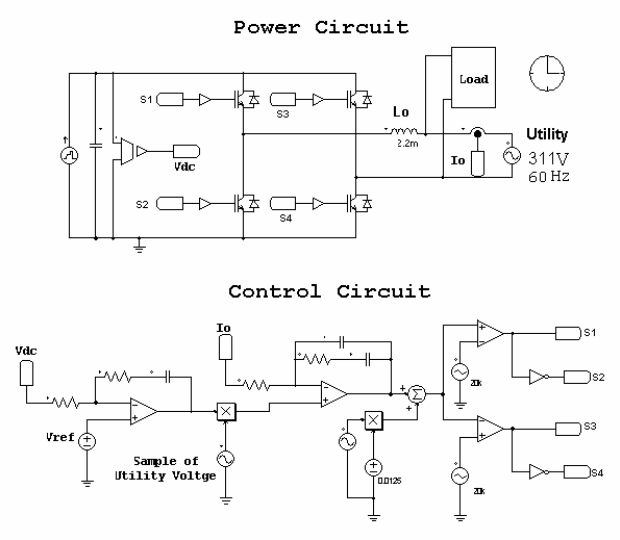

Fig. 14. Simulated Circuit.

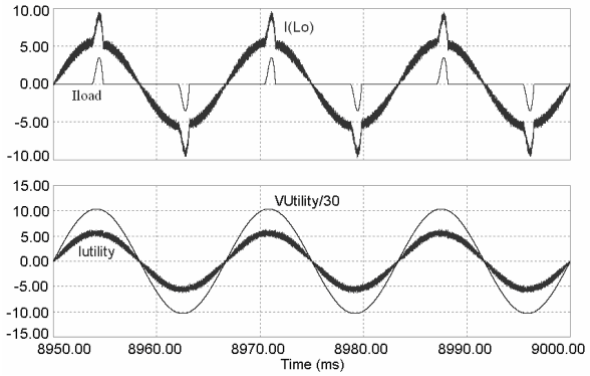

Fig. 15. Output inductor current (I_{Lo}) and nonlinear capacitive load current (I_{Load}), utility current ($I_{utility}$) and utility voltage ($V_{utility}$).

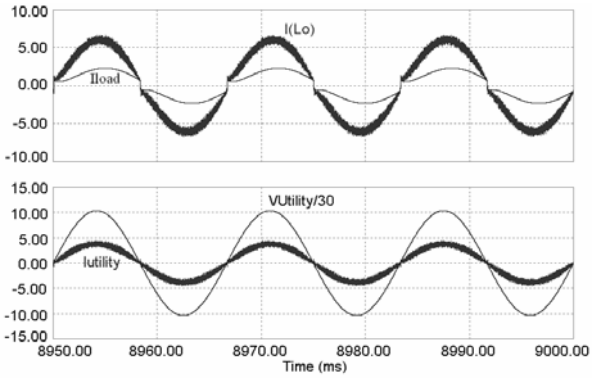

Fig. 16 Output inductor current (I_{Lo}) and nonlinear inductive load current (I_{Load}), utility current ($I_{utility}$) and utility voltage ($V_{utility}$).

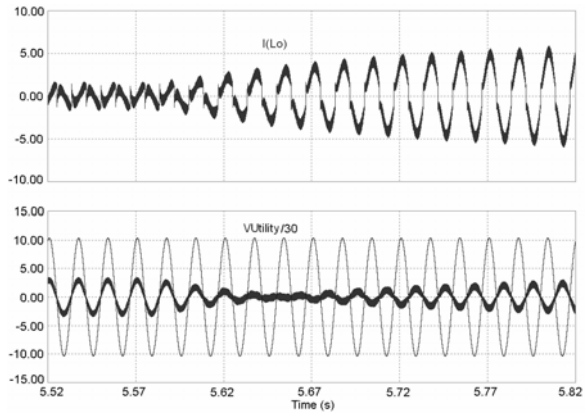

Fig. 17. System switching between solar generator mode and active power mode.